



## Research article

Nuciferine improves cardiac function in mice subjected to myocardial ischemia/reperfusion injury by upregulating PPAR- $\gamma$ Ruisha Li <sup>a,b,1</sup>, Xichun Qin <sup>a,b,1</sup>, Lijun Yue <sup>c</sup>, Wenxue Liu <sup>a,b</sup>, Yaxuan Gao <sup>a,b</sup>, Feng Zhu <sup>a,b</sup>, Dongjin Wang <sup>a,b,\*\*</sup>, Qing Zhou <sup>a,b,\*</sup><sup>a</sup> Department of Cardio-Thoracic Surgery, Nanjing Drum Tower Hospital, The Affiliated Hospital of Nanjing University Medical School, Nanjing, Jiangsu, China<sup>b</sup> Institute of Cardiothoracic Vascular Disease, Nanjing University, Nanjing, Jiangsu, China<sup>c</sup> Department of Traditional Chinese Medicine, Nanjing Drum Tower Hospital, The Affiliated Hospital of Nanjing University Medical School, Nanjing, Jiangsu, China

## ARTICLE INFO

## Keywords:

Nuciferine  
Ischemia/reperfusion  
Cardiomyocytes  
PPAR- $\gamma$ 

## ABSTRACT

Ischemic heart disease and myocardial infarction contribute to the leading cause of death in worldwide. The prevention and management of myocardial ischemia/reperfusion (I/R) injury is an essential part of coronary heart disease surgery and is becoming a major clinical problem in the treatment of ischemic heart disease. Nuciferine has potent anti-inflammatory and antioxidative stress effects, but its role in myocardial ischemia-reperfusion (I/R) is unclear. In this study, we found that nuciferine could reduce the myocardial infarct size in a mouse myocardial ischemia-reperfusion model and improve cardiac function. Furthermore, nuciferine could effectively inhibit hypoxia and reoxygenation (H/R) stimulated apoptosis of primary mouse cardiomyocytes. In addition, nuciferine significantly reduced the level of oxidative stress. The peroxisome proliferator-activated receptor gamma (PPAR- $\gamma$ ) inhibitor GW9662 could reverse the protective effect of nuciferine on cardiomyocytes. These results indicate that nuciferine can inhibit the apoptosis of cardiomyocytes by upregulating PPAR- $\gamma$  and reducing the I/R-induced myocardial injury in mice.

## 1. Introduction

Cardiovascular disease kills 17.8 million people worldwide and causes disability in 35.6 million people every year; thus, imposing a huge economic burden on countries around the world [1]. This not only affects high-income countries but also low- and middle-income countries [2]. Myocardial infarction is the main cause of death from cardiovascular events [3]. Timely and effective restoration of coronary blood flow is an effective method for the treatment of ischemic heart diseases, such as myocardial infarction. However, in the process of restoring the blood supply, damage is caused to the myocardial tissue structure, energy metabolism, electrophysiology, and

\* Corresponding author. Department of Cardio-Thoracic Surgery, The Affiliated Drum Tower Hospital of Nanjing University Medical School, Nanjing 210008, Jiangsu, China.

\*\* Corresponding author. Department of Cardio-Thoracic Surgery, Nanjing Drum Tower Hospital, The Affiliated Hospital of Nanjing University Medical School, Nanjing, Jiangsu, China.

E-mail addresses: [wangdongjin@njgly.com](mailto:wangdongjin@njgly.com) (D. Wang), [zhouqing@njgly.com](mailto:zhouqing@njgly.com) (Q. Zhou).

<sup>1</sup> These authors contributed equally to this work.

<https://doi.org/10.1016/j.heliyon.2023.e13630>

Received 12 September 2022; Received in revised form 1 February 2023; Accepted 6 February 2023

Available online 11 February 2023

2405-8440/© 2023 The Authors. Published by Elsevier Ltd. This is an open access article under the CC BY-NC-ND license (<http://creativecommons.org/licenses/by-nc-nd/4.0/>).

cardiac function. This phenomenon is called myocardial ischemia-reperfusion (I/R) injury [4–6].

Myocardial I/R injury usually leads to the following four types of myocardial dysfunction: myocardial stunning, no-reflow phenomenon, reperfusion arrhythmia, and fatal reperfusion injury [7]. Reducing the harm caused by I/R injury has become a hotspot and focus of cardiovascular research [8]. It is currently recognized that oxidative stress and inflammation are the two main mechanisms of I/R injury [9,10]. Excessive reactive oxygen species (ROS) production in the I/R process will cause a cascade of cardiac inflammation, which will cause further damage to the surviving cardiomyocytes [11]. Inhibition of inflammation and oxidative stress can reduce I/R injury and protect cardiac function [12,13]. Therefore, the development or exploration of new targets and drugs for myocardial protection represents a scientific and technological challenge in the medical field.

With the rapid development in the field of pharmacology, an increasing number of active compounds in natural products have been discovered [14]. Nuciferine is an alkaloid containing aromatic rings, which is extracted from lotus leaves. It has received extensive attention due to its unique pharmacological effects and low toxicity [15]. With in-depth research on nuciferine, it has been proven that it has a variety of biological activities, such as anti-inflammatory, antioxidant, antibacterial, and antitumor activities [16]. One study found that nuciferine protects against isoproterenol-induced myocardial infarction (MI) in rats, indicating the potential value of nuciferine in cardiovascular disease [17]. However, whether nuciferine can alleviate myocardial injury and reduce myocardial cell apoptosis after I/R is still unclear.

To date, there is insufficient evidence to prove the specific role of nuciferine in protection against I/R injury. Therefore, the purposes of this research were to 1) explore whether nuciferine can exert myocardial protection after ischemia and reperfusion and reduce myocardial cell damage and 2) explore the relevant mechanism by which nuciferine protects the cardiomyocytes.

## 2. Materials and methods

### 2.1. Mice and mouse myocardial I/R injury model

All animal studies were performed according to the Model Animal Research Center of Nanjing University. The experimental protocols were approved by the Animal Care and Use Committee of Nanjing University Medical School. C57BL/6J male mice (20 ± 2g, 8 weeks old) were reared in pathogen-free facilities (24 ± 2 °C and 45 ± 15% humidity with a 12/12 h light-dark cycle). Experimental mice were gavaged and treated with a nuciferine dose of 10 mg/kg in the treatment group at 4 h before model establishment [18]. After a week of acclimatization, mice were utilized to develop the myocardial I/R model, as previously described [19]. Briefly, mice were anesthetized by an intraperitoneal injection of sodium pentobarbital (45 mg/kg) and the heart was exposed through a left thoracic incision. Next, a 7.0-slip suture slip knot was ligated around the left anterior descending coronary artery (LAD) to induce myocardial infarction for 45 min. Mice were euthanized 24 h after perfusion. Mice in the sham-operated group underwent surgery to expose the heart, but LAD ligation was not performed.

### 2.2. Cardiac function evaluation

Two-dimensional-guided M-mode echocardiography was used to determine the left ventricular ejection fraction (LEF). Left ventricular end-diastolic volume (EDV) and end-systolic volume (ESV) were measured by Vevo2100 (Japan). The LEF was calculated as follows:  $EF = (EDV - ESV) / EDV * 100\%$ . All measurements were based on the average of at least 3 cardiac cycles.

### 2.3. Measurement of myocardial infarction (MI) size

Before harvesting the mouse heart, 1 mL of 0.5% Evans blue dye (E2129, Sigma) was injected into the ascending aorta. The mouse heart was placed in the refrigerator at −20 °C for 20 min, and then the left ventricle was cut into 2 mm thick slices perpendicular to the left anterior descending branch. Then, samples were immersed in 1% 2,3,5-triphenyltetrazolium (T8877, Sigma) in PBS at 37 °C for 10–15 min to differentiate between the infarcted tissue and viable myocardium. All sections were captured by ImageJ. The infarct area (%) was calculated by the ratio of the infarct area to the ischemic area.

### 2.4. Histologic assessment of myocardial tissue

The mouse hearts in each group were made into 10 μm thick frozen sections, and then they were stained with hematoxylin and eosin (H&E). The cross-sectional diameter of cardiomyocytes was determined by an optical microscope (DP74, Olympus). In each group, 15 to 20 images (including at least 50 cardiomyocytes) were captured to assess the cross-sectional area (CSA).

### 2.5. Cell culture and establishment of hypoxia-reoxygenation (H/R) model

Suckling mouse ventricular myocytes were isolated from the hearts of C57BL/6J mice (1 day). Hearts were digested, washed with HBSS buffer (Gibco, pH 7.4), predigested in 20 mL Tyrisin buffer (0.05%) for 1 h, and finally digested with 1 mg/mL collagenase II (17101015, Gibco) for incubation at 37 °C with constant agitation 3 times for 10 min. Supernatants were centrifuged at 1000 rpm for 5 min. Cultures were enriched with cardiac myocytes by preplating for 90 min to eliminate fibroblasts. Cardiac myocytes were resuspended in the medium (DMEM supplemented with 10% fetal bovine serum, 100 U/mL penicillin–streptomycin and cytarabine for injection). Cardiac myocytes were plated at a final density of  $1.0 \times 10^3 / \text{mm}^2$  on laminin-precoated culture dishes or coverslips. After

continuous culture for 2 days, for hypoxia, the cells were switched to DMEM without fetal bovine serum and placed in a trigas incubator adjusting 1% O<sub>2</sub> for 24 h [20]. After H/R, the cells were switched back to the regular culture media and placed in a normoxic incubator for another 3 h before harvest. Pre-incubation of cardiomyocytes with nuciferine (5  $\mu$ M) for 2 h prior to hypoxia in the nuciferine treatment group, which was clarified in Section Results.

## 2.6. CCK-8 analysis

The cells were seeded on 96-well plates and cultured in a humidified incubator containing 5% CO<sub>2</sub> at 37 °C. Briefly, incubated nuciferine was administered as needed for the experiment and the fresh culture medium containing CCK-8 (C0041, Beyotime) reagent (10:1) was added and cultured at 37 °C for another 2 h. Then, the samples were detected using a microplate reader (Multiskan GO, Thermo) at 450 nm.

## 2.7. Western blotting analysis

RIPA lysis buffer was used to extract total proteins from mouse cardiomyocytes and heart tissues. The bicinchoninic acid (BCA) kit was used to detect the concentration of protein. 10% SDS–PAGE was used to separate the cells or tissue lysate. After the protein transfer step, the PVDF membrane (ISEQ00010, Millipore) was sealed with 5% skim milk, and then pro-caspase3, cleaved caspase3 (9664, CST, USA) and  $\beta$ -tubulin were with anti-peroxisome proliferator-activated receptor gamma (PPAR- $\gamma$ ) (16643-1-AP, China, Proteintech) and Bax (ab32503, Abcam, UK). After washing three times in tributyltin compound buffer, the secondary antibody was incubated at room temperature for 1 h. Finally, ECL solution (KGP112, Jiangsu Kechuang Biotechnology Co., Ltd., China) was used to visualize the protein. Blots were analyzed using the Tanon image system (Tanon-1600, Tanon).

## 2.8. Terminal deoxynucleotidyl transferase dUTP nick end labeling (TUNEL) staining for apoptosis

Samples were prepared using the TUNEL Bright Green Apoptosis Detection Kit (A112-01, Vazyme, China) based on the manufacturer's instructions. Briefly, samples were washed twice in PBS, and 0.3% Triton X-100 was used to permeate the cells after they were fixed for 15 min using 4% paraformaldehyde. Finally, the TUNEL detection solution was added to the samples and incubated for 60 min in a 37 °C incubator protected from light. TUNEL-positive cells were counted using an FV3000 microscope (Olympus).

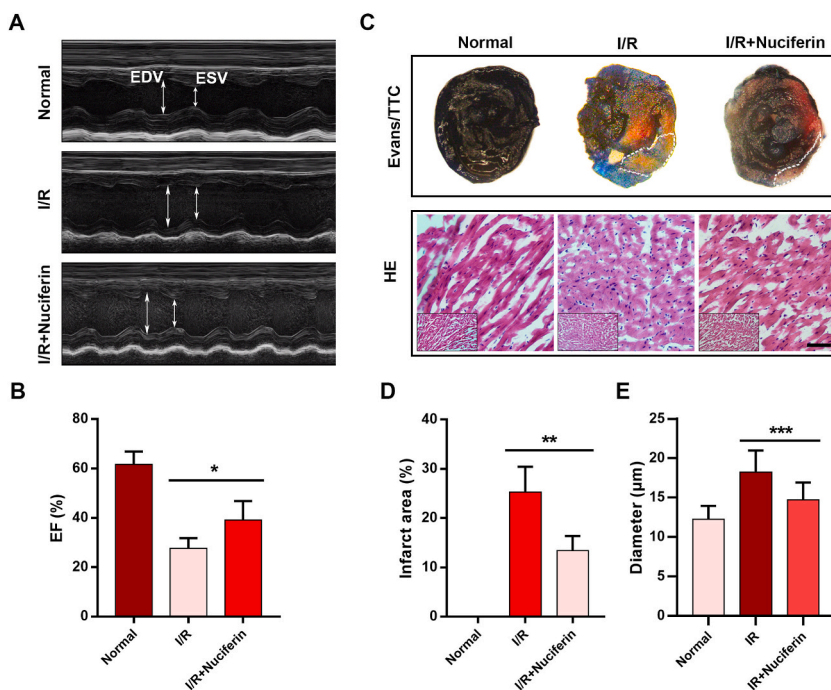


**Fig. 1.** Nuciferine improves cardiac function and reduces myocardial infarction size in I/R mice. (A) The left ventricular ejection fraction (EF%) was measured by transthoracic M-mode echocardiography. (B) Quantitative statistics of EF%. (C) Representative images of the Evans blue/2,3,5-triphenyltetrazolium staining and HE staining of myocardial tissues. Bar = 50  $\mu$ m. (D) Quantitative analysis of the infarct size in each group. (E) Quantitative analysis of the cardiomyocyte diameter in each group. Data are expressed as the mean  $\pm$  SD, n = 5, \* $P$  < 0.05, \*\* $P$  < 0.01, \*\*\* $P$  < 0.001 vs. the indicated group. (For interpretation of the references to colour in this figure legend, the reader is referred to the Web version of this article.)

## 2.9. Immunofluorescence and immunohistochemistry (IHC) staining

The samples were fixed with 4% paraformaldehyde for 15 min, permeabilized with Triton X-100 (0.1%), and blocked with a solution containing 5% bovine serum for 1 h before primary antibody application. Samples were incubated with anti-mouse cTnT or PPAR- $\gamma$  antibody for 12 h at 4 °C and secondary antibody for 1 h at room temperature in the dark. Nuclei were stained with DAPI (MBD0015, Sigma). The sections for IHC incubated with HRP polymer-conjugated secondary antibody at room temperature for 15–30 min. Then, the sections were stained with hematoxylin and eosin. After the final wash with PBS, the samples were observed under a fluorescence microscope (Olympus).

## 2.10. Detection of the intracellular ROS and superoxide dismutase (SOD) activity

ROS and SOD activities were assessed in all experimental groups using the ROS and SOD activity assay kits.

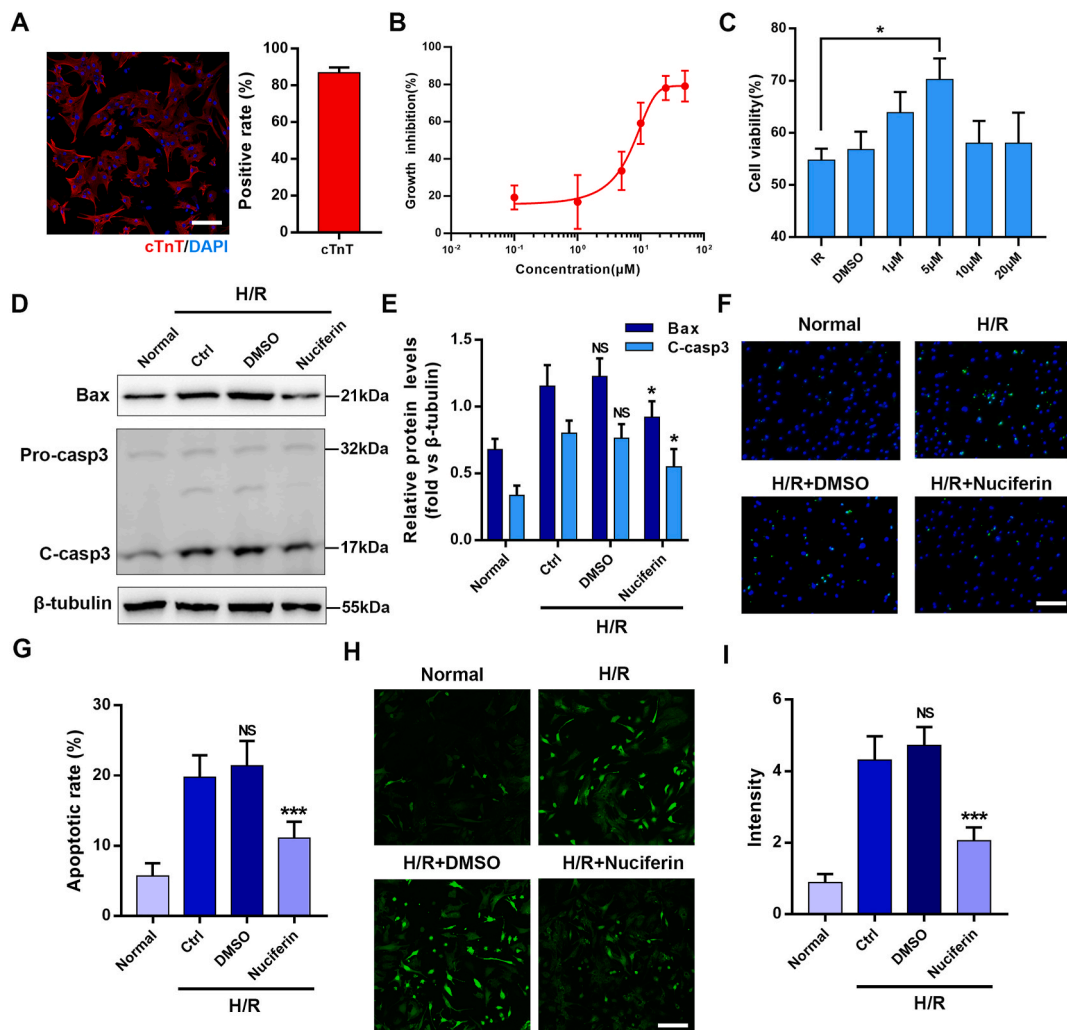


**Fig. 2.** Nuciferine reduces cardiomyocyte apoptosis and ROS level. (A) Identification of cardiomyocytes using fluorescence microscope and quantitative statistics of the positive rate of cTnT. Bar = 100  $\mu$ m. (B) The effect of different concentrations of nuciferine on cardiomyocytes. (C) The effect of different concentrations of nuciferine on cell survival in the primary cardiomyocyte H/R model. (D) Western blotting to detect the effect of nuciferine on the expression of bax and c-casp3 (cleaved-caspase3) in cardiomyocyte H/R model after pre-incubation of myocytes with nuciferine (5  $\mu$ M) for 2 h. (E) Quantification of the related protein expression. (F) Representative images of TUNEL staining of primary cardiomyocytes in each indicated experimental condition. Bar = 100  $\mu$ m. (G) Quantitative analysis of cardiomyocyte apoptosis. (H) Representative images of ROS levels. Bar = 50  $\mu$ m. (I) Quantification of the ROS level. Data are expressed as the mean  $\pm$  SD. n = 3. NS,  $P > 0.05$ ; \*\*\* $P < 0.001$  vs. the normal group.

2.11. Statistical analysis

Data are presented as mean  $\pm$  standard deviation (SD). Multiple group comparisons were assessed using one-way ANOVA, followed by post hoc analysis using the least significant difference *t*-test. Data were compared between two independent groups using a two-tailed Student's *t*-test. Analysis was performed using SPSS 20 software (Chicago, IL, USA). Differences at  $P < 0.05$  were considered statistically significant.

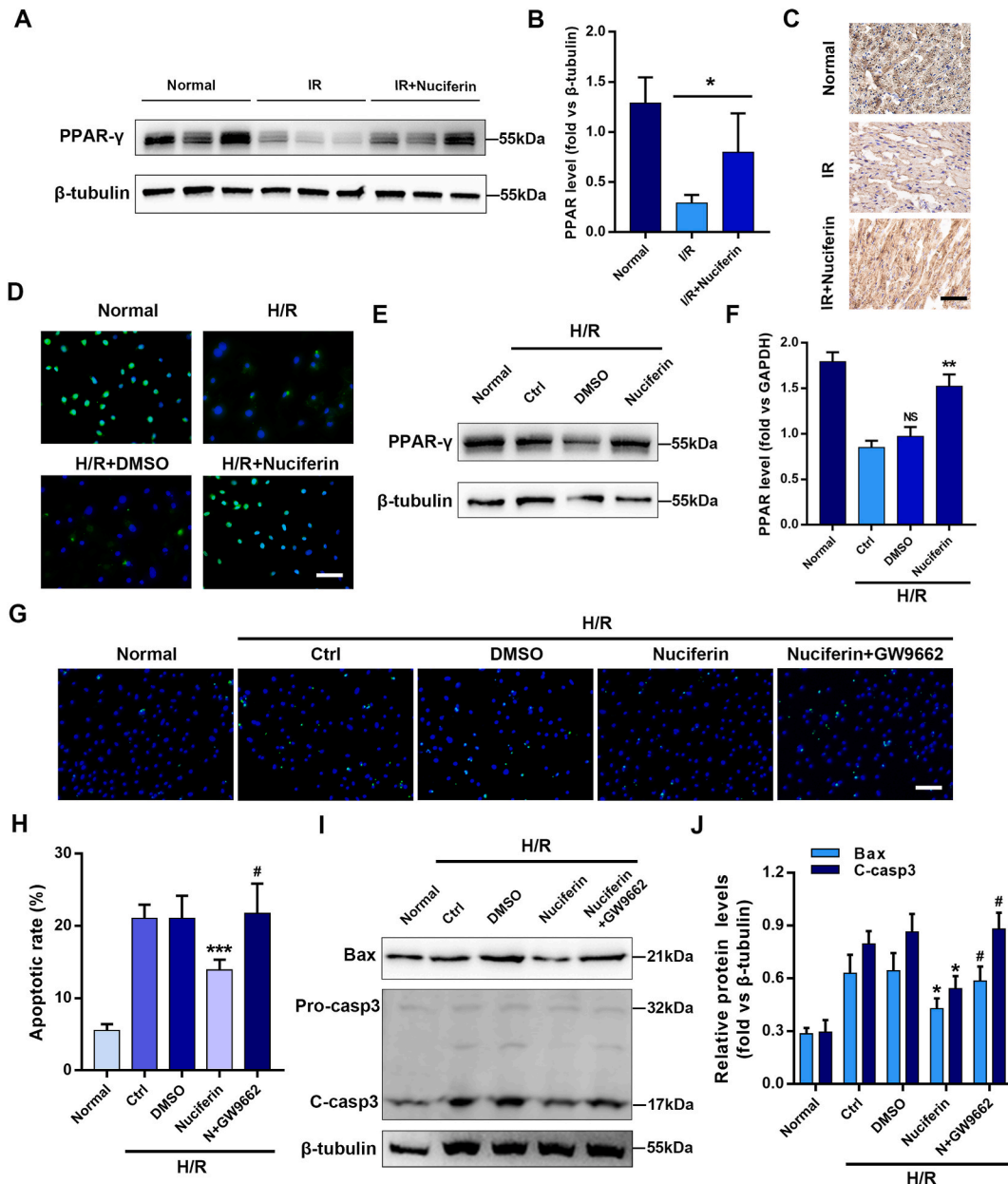


**Fig. 3.** Nuciferine reduces cardiomyocyte apoptosis by upregulating PPAR- $\gamma$  activity. (A) Western blotting to detect the effect of nuciferine on the expression of PPAR- $\gamma$  in mouse myocardial tissue. (B) Quantification of the PPAR- $\gamma$  expression. (C) Immunohistochemistry representative images of PPAR- $\gamma$  expression in mouse myocardial tissue. Bar = 200  $\mu$ m. (D) Immunofluorescence representative images of PPAR- $\gamma$  expression in cardiomyocyte. Bar = 100  $\mu$ m. (E) Western blotting to detect the effect of nuciferine on the expression of PPAR- $\gamma$  *in vitro*. (F) Quantification of the PPAR- $\gamma$  expression. (G) Representative images of TUNEL staining of primary cardiomyocytes with or without PPAR- $\gamma$  inhibitors (GW 9662). Bar = 50  $\mu$ m. (H) Quantitative analysis of cardiomyocyte apoptosis. (I) Western blotting to detect the effect of nuciferine on the expression of bax and c-casp3 in each indicated experimental condition. (J) Quantification of the related protein expression. Data are expressed as the mean  $\pm$  SD.  $n = 3$ . \* $P < 0.05$ ; \*\*\* $P < 0.001$  vs. the control group. # $P < 0.05$  vs. the nuciferine group.



### 3. Results

#### 3.1. Nuciferine reduces myocardial infarction and myocardial cell damage and improves cardiac function

Myocardial I/R can cause cardiomyocyte apoptosis and cardiac dysfunction. The degree of I/R-induced cardiac function damage was measured by the transthoracic 2-dimensional-guided M-mode. After the myocardium was subjected to ischemia and hypoxia for up to 45 min and subsequent 24 h of reperfusion, the mouse cardiac function decreased from  $61.69 \pm 5.20\%$  to  $27.74 \pm 4.07\%$ . After receiving nuciferine treatment, heart function increased to  $39.07 \pm 7.74\%$  (Fig. 1A and B). This suggested that nuciferine could significantly improve the heart function. Next, we measured the area of myocardial infarction in mice by Evas/TTC staining. Consistent with the cardiac function results, nuciferine effectively reduced the area of myocardial infarction ( $25.25 \pm 5.18\%$  vs.  $13.41 \pm 2.97\%$ ) in mice (Fig. 1C and D). In addition, we also investigated the effects of I/R on cardiomyocyte edema by histological analysis. The results of cardiomyocyte diameter measurement showed that cardiomyocytes in the infarcted area showed severe edema, and after nuciferine treatment, cardiomyocyte morphology recovered significantly (Fig. 1C and E). These results indicated that nuciferine could reduce myocardial cell damage and improve cardiac function in mice subjected to ischemia and reperfusion.

#### 3.2. Establishment of the H/R model of cardiomyocytes

The safety of nuciferine has been demonstrated in numerous prior studies. To confirm this, we isolated primary cardiomyocytes from neonatal mouse myocardium, tested the purity of cardiomyocytes by immunofluorescence. The results (Fig. 2A) showed that the cTnT positive rate of cardiomyocytes was about 90% ( $86.9 \pm 3.0\%$ ). Then we used CCK-8, a sensitive cell viability determination method, to evaluate the toxicity of nuciferine in cardiomyocytes at different concentrations. After treatment for 48 h, across a 0.1–50  $\mu\text{M}$  range of concentrations, nuciferine had no obvious toxic effect on cardiomyocytes at concentrations below 10  $\mu\text{M}$ , and this result would guide the subsequent experiments (Fig. 2B). Next, to investigate the effects of nuciferine on cardiomyocytes exposed to H/R, the levels of cell viability were evaluated in cardiomyocytes at different concentrations of nuciferine. Different concentrations of nuciferine had different effects on the viability of H/R-exposed cardiomyocytes (Fig. 2C). According to this result, the concentration of nuciferine was set at 5  $\mu\text{M}$  for subsequent drug effect experiments.

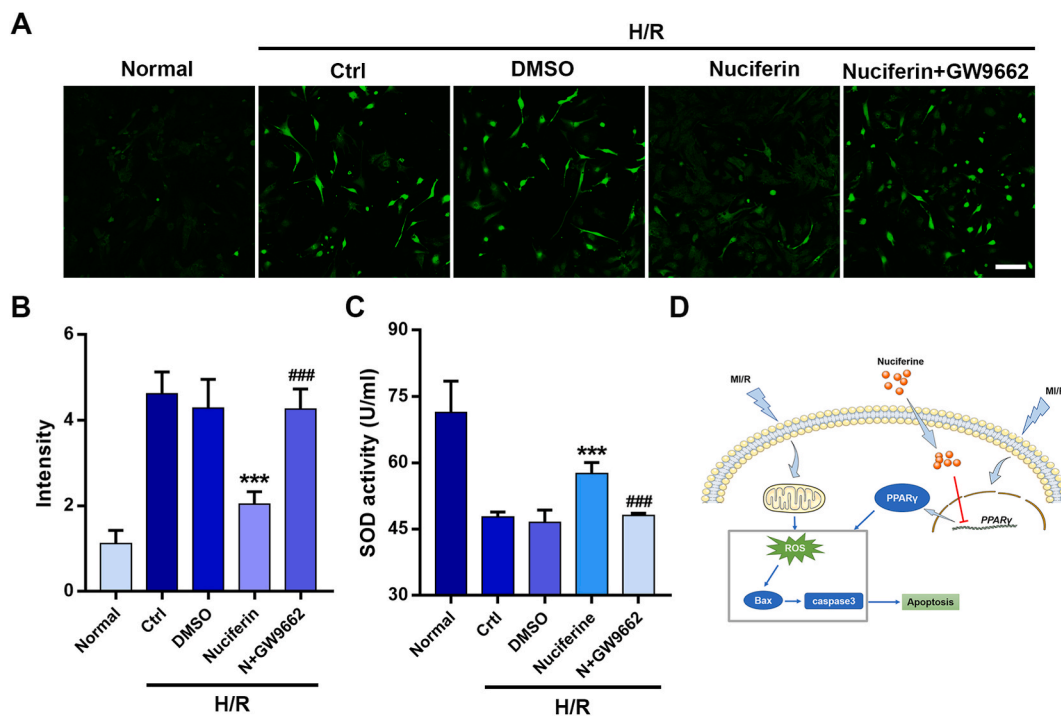


**Fig. 4.** Nuciferine reduces the oxidative stress level by upregulating PPAR- $\gamma$  activity. (A) Representative images of ROS levels. Bar = 50  $\mu\text{m}$ . (B) Quantification of the ROS level. (C) Quantification of the SOD level. Data are expressed as the mean  $\pm$  SD.  $n = 4$ . \*\*\* $P < 0.001$  vs. the control group. ### $P < 0.001$  vs. the nuciferine group. (D) Schematic diagram demonstrating that nuciferine inhibited apoptosis of cardiomyocytes by upregulating the activity of PPAR- $\gamma$ .

### 3.3. Nuciferine reduces cardiomyocyte apoptosis and ROS production

To further determine the protective effect of nuciferine on cardiomyocytes, after pre-incubation of myocytes with nuciferine for 2 h, we established the H/R model and detected cardiomyocyte damage and apoptosis. The results showed that treatment with nuciferine could significantly reduce the levels of bax and cleaved caspase-3 compared with those in the H/R group (Fig. 2D and E). Then, we used TUNEL staining to further confirm the apoptosis of cardiomyocytes (Fig. 2F and G). The results suggested similar trends; i.e., nuciferine could effectively reduce cardiomyocyte apoptosis. These observations indicated that nuciferine prevented H/R-induced cardiomyocyte apoptosis. In addition, we also investigated the production of ROS, which is a key factor in myocardial I/R injury (Fig. 2H and I). The results showed that nuciferine significantly reduced the generation of ROS, which might be an important factor in protecting the cardiomyocytes and reducing their apoptosis.

### 3.4. Nuciferine inhibits ROS generation and reduces cardiomyocyte apoptosis by upregulating PPAR- $\gamma$

After demonstrating the protective effect of nuciferine on H/R-induced cardiomyocyte apoptosis, we investigated the mechanism of its biological function. PPAR- $\gamma$  is a transcription factor that can heterodimerize with retinoid X receptors and activate genes involved in lipid homeostasis [21]. One study showed that nuciferine activated PPAR- $\gamma$ , thereby inhibiting lipopolysaccharide (LPS)-induced inflammatory damage in BV2 cells [22]. It was determined whether nuciferine upregulates the activity of cardiomyocyte PPAR- $\gamma$  and reduces the apoptosis. Consistent with our expectations, we found that PPAR- $\gamma$  expression was decreased in the myocardial tissue of I/R model mice, and nuciferine played a role in stabilizing PPAR- $\gamma$  expression (Fig. 3A–C). Similarly, after H/R treatment, the PPAR- $\gamma$  expression of cardiomyocytes was reduced significantly, and nuciferine reversed this change (Fig. 3D–F). The quantitative results of cleaved caspase3 and bax and TUNEL staining further proved that the inhibitor GW9662 (PPAR- $\gamma$  ligand binding domain antagonist) could reverse the protective effect of nuciferine on cardiomyocytes (Fig. 3G–J). Similarly, the inhibitor GW9662 was able to increase H/R injury-induced ROS generation, and inhibit SOD levels (Fig. 4A–C). In summary, these findings suggested that nuciferine promoted cardiomyocyte survival by upregulating PPAR- $\gamma$ .

## 4. Discussion

In this study, nuciferine was proven to reduce the myocardial infarct size in a mouse myocardial I/R model and improve cardiac function. In addition, we explored its potential biological functional mechanisms: nuciferine reduces the production of ROS by upregulating PPAR- $\gamma$ , thereby reducing I/R-induced cardiomyocyte damage (Fig. 4D).

Emergency recovery of coronary artery patency through anticoagulants, thrombolytics, and percutaneous coronary intervention is the gold standard for patients with acute myocardial infarction [23]. Timely reperfusion is essential to alleviate ischemic injury and save viable cardiomyocytes. However, immediate reperfusion after prolonged ischemia has been shown to often accelerate the process of cell death and increase the degree of infarction [24]. Therefore, there is an increasing need for new treatment strategies to limit the extent of myocardial infarction caused by I/R injury. During reperfusion, when O<sub>2</sub> is reperused into the ischemic site, it will cause the upregulation and activation of NOX and then generate ROS [25]. ROS can mediate the infiltration of neutrophils and further activate NOX to promote the production of ROS [26]. Excessive ROS can affect the permeability of cell membranes, cause oxidative damage to specific molecules inside, and cause irreversible cell damage, which is the main driving factor leading to myocardial I/R injury [27]. In addition, ROS can also promote inflammatory signal transduction, regulate myocardial cell apoptosis, and participate in myocardial remodeling after myocardial infarction [28]. PPAR- $\gamma$  is an important transcription regulator that regulates several key enzymes related to lipid metabolism and has a variety of biological functions, such as anti-inflammatory, antioxidant, antiapoptotic, and antihypertensive activities [21]. Accumulating evidence has suggested the importance of PPAR- $\gamma$  in preventing myocardial I/R injury due to its role in upregulating adiponectin synthesis [29]. As inflammation has been widely recognized to play an important role in aggravating I/R injury, the activation of PPAR- $\gamma$  via thiazolidinediones, such as rosiglitazone and troglitazone, has been demonstrated to inhibit nuclear factor kappa B (NF- $\kappa$ B) activation and release of pro-inflammatory cytokines, such as tumor necrosis factor  $\alpha$  (TNF- $\alpha$ ), in cardiomyocytes [30]. Similarly, upregulating the activity of PPAR- $\gamma$  can reduce the production of ROS, thereby saving dying cardiomyocytes [31].

The anti-inflammatory effects of nuciferine have been reported in a variety of disease models. For example, nuciferine has been proved to play a protective role on fructose-induced renal injury in rats by inhibiting the TLR4/PI3K/NF- $\kappa$ B pathway and NLRP3 inflammasome activation [32]. Nuciferine also inhibited hyperuricemia and kidney damage induced by potassium oxysulfide in mice by regulating renal organic ion transporters and inflammatory reaction [18]. It also has a certain protective effect on isoproterenol-induced myocardial infarction [17]. However, it is not clear whether nuciferine has a beneficial effect in myocardial I/R injury. Our results showed that nuciferine upregulated the cardiomyocyte PPAR- $\gamma$  expression during H/R, which might be an important reason for reducing ROS generation. It is not clear how nuciferine causes an increase in PPAR- $\gamma$  activity. Studies on the biological activity of nuciferine suggested that there might be multiple receptors on the membrane and multiple intracellular signal transduction pathways. The target and mechanism of nuciferine still need to be further explored.

## 5. Conclusion

Our results indicated that nuciferine could be used as a protective factor for cardiomyocytes after I/R. The application of nuciferine during myocardial I/R is a feasible strategy to reduce cardiomyocyte apoptosis and improve cardiac function. These findings provide a

promising and prospective method for improving myocardial I/R management and prognosis strategies.

### Ethics approval and consent to participate

The study was conducted in accordance with the ARRIVE guidelines and animal experiments were carried out in accordance with the guide for the Care and Use of Laboratory Animals published by the US National Institutes of Health (NIH Publication, 8th Edition, 2011).

### Author contribution statement

Ruisha Li, Xichun Qin: Conceived and designed the experiments; Performed the experiments; Analyzed and interpreted the data; Wrote the paper.

Lijun Yue, Wenxue Liu, Yaxuan Gao, Feng Zhu: Analysis tools or data; Performed the experiments; Analyzed and interpreted the data; Wrote the paper.

Dongjin Wang, Qing Zhou: Conceived and designed the experiments; Contributed reagents, materials; Wrote the paper.

### Funding statement

Dongjin Wang was supported by National Natural Science Foundation of China [81970401].

### Data availability statement

Data included in article/supp. material/referenced in article.

### Declaration of interest's statement

The authors declare no competing interests.

### Acknowledgment

Not applicable.

### Appendix A. Supplementary data

Supplementary data to this article can be found online at <https://doi.org/10.1016/j.heliyon.2023.e13630>.

### References

- [1] G.A. Mensah, G.A. Roth, V. Fuster, The global burden of cardiovascular diseases and risk factors: 2020 and beyond, *J. Am. Coll. Cardiol.* 74 (2019) 2529–2532. <https://doi.org/10.1016/j.jacc.2019.10.009>.
- [2] G.A. Roth, G.A. Mensah, C.O. Johnson, G. Addolorato, E. Ammirati, L.M. Baddour, N.C. Barengo, A.Z. Beaton, E.J. Benjamin, C.P. Benziger, A. Bonny, M. Brauer, M. Brodmann, T.J. Cahill, J. Carapetis, A.L. Catapano, S.S. Chugh, L.T. Cooper, J. Coresh, M. Criqui, N. DeCleene, K.A. Eagle, S. Emmons-Bell, V.L. Feigin, J. Fernandez-Sola, G. Fowkes, E. Gakidou, S.M. Grundy, F.J. He, G. Howard, F. Hu, L. Inker, G. Karthikeyan, N. Kassebaum, W. Koroshetz, C. Lavie, D. Lloyd-Jones, H.S. Lu, A. Mirijello, A.M. Temesgen, A. Mokdad, A.E. Moran, P. Muntner, J. Narula, B. Neal, M. Ntsekhe, G. Moraes de Oliveira, C. Otto, M. Owolabi, M. Pratt, S. Rajagopalan, M. Reitsma, A.L.P. Ribeiro, N. Rigotti, A. Rodgers, C. Sable, S. Shakil, K. Sliwa-Hahnle, B. Stark, J. Sundstrom, P. Timpel, I.M. Tleyjeh, M. Valgimigli, T. Vos, P.K. Whelton, M. Yacoub, L. Zuhlke, C. Murray, V. Fuster, G.-N.-J.G.B.o.C.D.W. Group, Global burden of cardiovascular diseases and risk factors, 1990–2019: update from the GBD 2019 study, *J. Am. Coll. Cardiol.* 76 (2020) 2982–3021. <https://doi.org/10.1016/j.jacc.2020.11.010>.
- [3] G. Damiani, E. Salvatori, G. Silvestrini, I. Ivanova, L. Bojovic, L. Iodice, W. Ricciardi, Influence of socioeconomic factors on hospital readmissions for heart failure and acute myocardial infarction in patients 65 years and older: evidence from a systematic review, *Clin. Interv. Aging* 10 (2015) 237–245. <https://doi.org/10.2147/CIA.S71165>.
- [4] D.P. Del Re, D. Amgalan, A. Linkermann, Q. Liu, R.N. Kitsis, Fundamental mechanisms of regulated cell death and implications for heart disease, *Physiol. Rev.* 99 (2019) 1765–1817. <https://doi.org/10.1152/physrev.00022.2018>.
- [5] Q. Fan, R. Tao, H. Zhang, H. Xie, L. Lu, T. Wang, M. Su, J. Hu, Q. Zhang, Q. Chen, Y. Iwakura, W. Shen, R. Zhang, X. Yan, Dectin-1 contributes to myocardial ischemia/reperfusion injury by regulating macrophage polarization and neutrophil infiltration, *Circulation* 139 (2019) 663–678. <https://doi.org/10.1161/CIRCULATIONAHA.118.036044>.
- [6] X. Chang, A. Lochner, H.H. Wang, S. Wang, H. Zhu, J. Ren, H. Zhou, Coronary microvascular injury in myocardial infarction: perception and knowledge for mitochondrial quality control, *Theranostics* 11 (2021) 6766–6785. <https://doi.org/10.7150/thno.60143>.
- [7] R. Ferreira, The reduction of infarct size—forty years of research—second of two parts, *Rev. Port. Cardiol.* 29 (2010) 1219–1244.
- [8] H. Zhu, Y. Tan, W. Du, Y. Li, S. Toan, D. Mui, F. Tian, H. Zhou, Phosphoglycerate mutase 5 exacerbates cardiac ischemia-reperfusion injury through disrupting mitochondrial quality control, *Redox Biol.* 38 (2021), 101777. <https://doi.org/10.1016/j.redox.2020.101777>.
- [9] G. Ndrepepa, Myeloperoxidase - a bridge linking inflammation and oxidative stress with cardiovascular disease, *Clin. Chim. Acta* 493 (2019) 36–51. <https://doi.org/10.1016/j.cca.2019.02.022>.
- [10] R. Wang, M. Wang, J. Zhou, D. Wu, J. Ye, G. Sun, X. Sun, Saponins in Chinese herbal medicine exerts protection in myocardial ischemia-reperfusion injury: possible mechanism and target analysis, *Front. Pharmacol.* 11 (2020), 570867. <https://doi.org/10.3389/fphar.2020.570867>.



- [11] J. Zhao, J. Zhang, Q. Liu, Y. Wang, Y. Jin, Y. Yang, C. Ni, L. Zhang, Hongjingtian injection protects against myocardial ischemia reperfusion-induced apoptosis by blocking ROS induced autophagic- flux, *Biomed. Pharmacother.* 135 (2021), 111205. <https://doi.org/10.1016/j.biopha.2020.111205>.
- [12] M.Y. Wu, G.T. Yang, W.T. Liao, A.P. Tsai, Y.L. Cheng, P.W. Cheng, C.Y. Li, C.J. Li, Current mechanistic concepts in ischemia and reperfusion injury, *Cell. Physiol. Biochem.* 46 (2018) 1650–1667. <https://doi.org/10.1159/000489241>.
- [13] L. Minutoli, D. Puzzolo, M. Rinaldi, N. Irrera, H. Marini, V. Arcoraci, A. Bitto, G. Crea, A. Pisani, F. Squadrito, V. Trichilo, D. Bruschetta, A. Micali, D. Altavilla, ROS-mediated NLRP3 inflammasome activation in brain, heart, kidney, and testis ischemia/reperfusion injury, *Oxid. Med. Cell. Longev.* 2016 (2016), 2183026. <https://doi.org/10.1155/2016/2183026>.
- [14] H. Wu, G. Zhao, K. Jiang, X. Chen, Z. Zhu, C. Qiu, C. Li, G. Deng, Plantamajoside ameliorates lipopolysaccharide-induced acute lung injury via suppressing NF-kappaB and MAPK activation, *Int. Immunopharm.* 35 (2016) 315–322. <https://doi.org/10.1016/j.intimp.2016.04.013>.
- [15] X. Chen, X. Zheng, M. Zhang, H. Yin, K. Jiang, H. Wu, A. Dai, S. Yang, Nuciferine alleviates LPS-induced mastitis in mice via suppressing the TLR4-NF-kappaB signaling pathway, *Inflamm. Res.* 67 (2018) 903–911. <https://doi.org/10.1007/s00011-018-1183-2>.
- [16] B.R. Sharma, L.N. Gautam, D. Adhikari, R. Karki, A comprehensive review on chemical profiling of *Nelumbo nucifera*: potential for drug development, *Phytother. Res.* 31 (2017) 3–26. <https://doi.org/10.1002/ptr.5732>.
- [17] R. HarishKumar, C.I. Selvaraj, Nuciferine from *Nelumbo nucifera* Gaertn. attenuates isoproterenol-induced myocardial infarction in Wistar rats, *Biotechnol. Appl. Biochem.* 69 (2021) 1176–1189. <https://doi.org/10.1002/bab.2194>.
- [18] D. Li, B. Liu, Y. Fan, M. Liu, B. Han, Y. Meng, X. Xu, Z. Song, X. Liu, Q. Hao, X. Duan, A. Nakai, Y. Chang, P. Cao, K. Tan, Nuciferine protects against folic acid-induced acute kidney injury by inhibiting ferroptosis, *Br. J. Pharmacol.* 178 (2021) 1182–1199. <https://doi.org/10.1111/bph.15364>.
- [19] N. Ale-Agha, P. Jakobs, C. Goy, M. Zurek, J. Rosen, N. Dyballa-Rukes, S. Metzger, J. Greulich, F. von Ameln, O. Eckermann, K. Unfried, F. Brack, M. Grandoch, M. Thielmann, M. Kamler, N. Gedik, P. Kleinbongard, A. Heinen, G. Heusch, A. Godecke, J. Altschmied, J. Haendeler, Mitochondrial telomerase reverse transcriptase protects from myocardial ischemia/reperfusion injury by improving complex I composition and function, *Circulation* 144 (2021) 1876–1890. <https://doi.org/10.1161/CIRCULATIONAHA.120.051923>.
- [20] Y. Fujio, T. Nguyen, D. Wencker, R.N. Kitsis, K. Walsh, Akt promotes survival of cardiomyocytes in vitro and protects against ischemia-reperfusion injury in mouse heart, *Circulation* 101 (2000) 660–667. <https://doi.org/10.1161/01.cir.101.6.660>.
- [21] C. Janani, B.D. Ranjitha Kumari, PPAR gamma gene—a review, *Diabetes Metabol. Syndr.* 9 (2015) 46–50. <https://doi.org/10.1016/j.dsx.2014.09.015>.
- [22] L. Zhang, J. Gao, P. Tang, L. Chong, Y. Liu, P. Liu, X. Zhang, L. Chen, C. Hou, Nuciferine inhibits LPS-induced inflammatory response in BV2 cells by activating PPAR-gamma, *Int. Immunopharm.* 63 (2018) 9–13. <https://doi.org/10.1016/j.intimp.2018.07.015>.
- [23] Y. Saito, Y. Kobayashi, Update on antithrombotic therapy after percutaneous coronary intervention, *Intern. Med.* 59 (2020) 311–321. <https://doi.org/10.2169/internalmedicine.3685-19>.
- [24] D.J. Hearse, R. Bolli, Reperfusion induced injury: manifestations, mechanisms, and clinical relevance, *Cardiovasc. Res.* 26 (1992) 101–108. <https://doi.org/10.1093/cvr/26.2.101>.
- [25] A.T. Turer, J.A. Hill, Pathogenesis of myocardial ischemia-reperfusion injury and rationale for therapy, *Am. J. Cardiol.* 106 (2010) 360–368. <https://doi.org/10.1016/j.amjcard.2010.03.032>.
- [26] Y.M. Kim, S.J. Kim, R. Tatsunami, H. Yamamura, T. Fukai, M. Ushio-Fukai, ROS-induced ROS release orchestrated by Nox4, Nox2, and mitochondria in VEGF signaling and angiogenesis, *Am. J. Physiol. Cell Physiol.* 312 (2017) C749–C764. <https://doi.org/10.1152/ajpcell.00346.2016>.
- [27] S. Cadenas, ROS and redox signaling in myocardial ischemia-reperfusion injury and cardioprotection, *Free Radic. Biol. Med.* 117 (2018) 76–89. <https://doi.org/10.1016/j.freeradbiomed.2018.01.024>.
- [28] Z.Q. Zhao, Oxidative stress-elicited myocardial apoptosis during reperfusion, *Curr. Opin. Pharmacol.* 4 (2004) 159–165. <https://doi.org/10.1016/j.coph.2003.10.010>.
- [29] S. Cuzzocrea, Peroxisome proliferator-activated receptors gamma ligands and ischemia and reperfusion injury, *Vasc. Pharmacol.* 41 (2004) 187–195. <https://doi.org/10.1016/j.vph.2004.10.004>.
- [30] H. Takano, T. Nagai, M. Asakawa, T. Toyozaki, T. Oka, I. Komuro, T. Saito, Y. Masuda, Peroxisome proliferator-activated receptor activators inhibit lipopolysaccharide-induced tumor necrosis factor-alpha expression in neonatal rat cardiac myocytes, *Circ. Res.* 87 (2000) 596–602. <https://doi.org/10.1161/01.res.87.7.596>.
- [31] A. Morrison, J. Li, PPAR-gamma and AMPK—advantageous targets for myocardial ischemia/reperfusion therapy, *Biochem. Pharmacol.* 82 (2011) 195–200. <https://doi.org/10.1016/j.bcp.2011.04.004>.
- [32] J. Xu, A. Ying, T. Shi, Nuciferine inhibits skin cutaneous melanoma cell growth by suppressing TLR4/NF-kappaB signaling, *Anti Cancer Agents Med. Chem.* 20 (2020) 2099–2105. <https://doi.org/10.2174/187152062066200811114607>.